

D10488

ADVMEW
ISSN 0935-9648
Vol. 20, No. 18
September 17, 2008

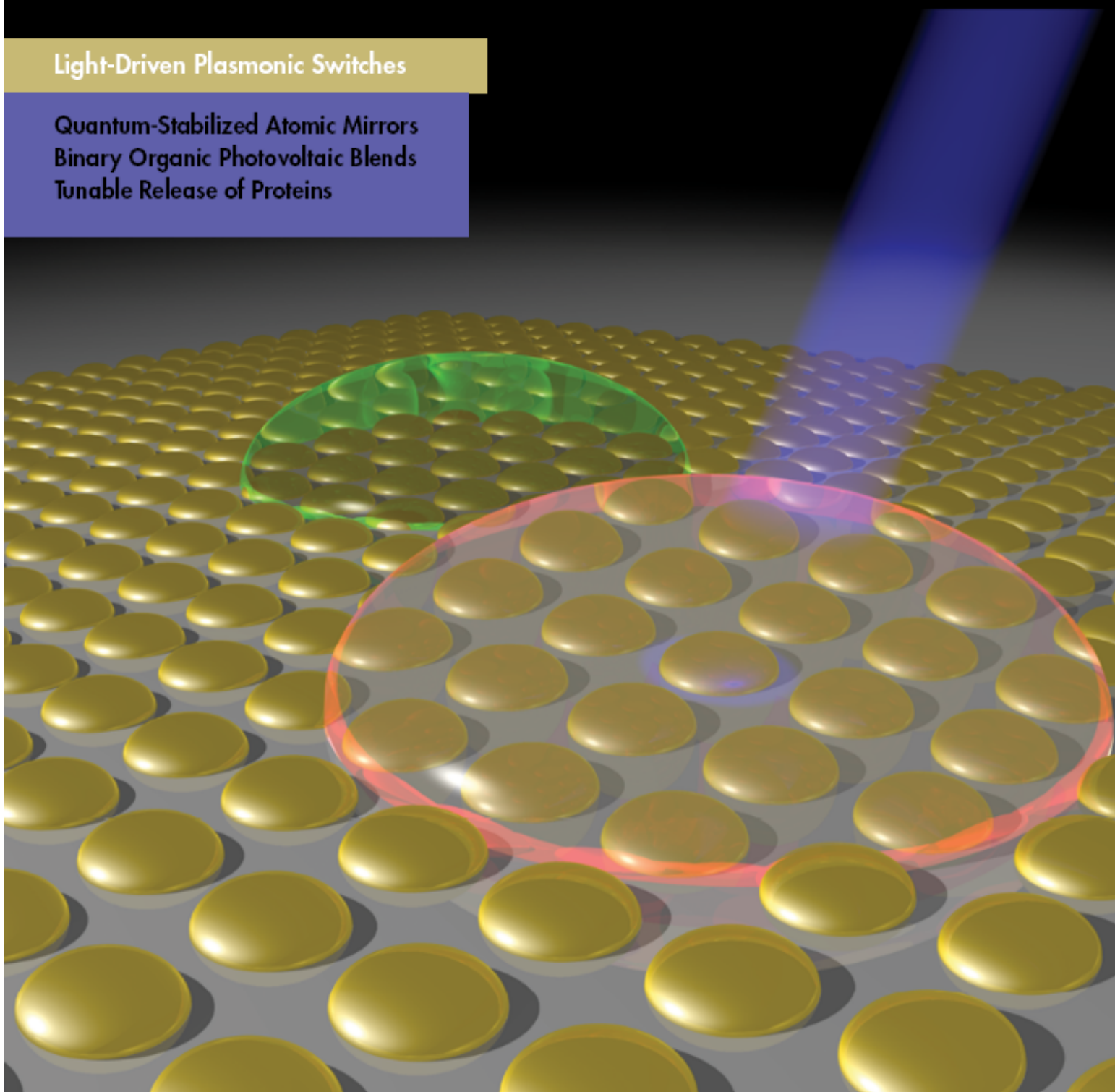


WILEY-
VCH

ADVANCED MATERIALS

Light-Driven Plasmonic Switches

Quantum-Stabilized Atomic Mirrors
Binary Organic Photovoltaic Blends
Tunable Release of Proteins



Light-Driven Plasmonic Switches Based on Au Nanodisk Arrays and Photoresponsive Liquid Crystals**

By Vincent K. S. Hsiao, Yue Bing Zheng, Bala Krishna Juluri, and Tony Jun Huang*

Surface plasmons are electromagnetic waves that oscillate collectively at a metal/dielectric interface.^[1] Because of its capability to localize and guide light in sub-wavelength metallic structures, surface-plasmon-based photonics, or “plasmonics”, offers an opportunity to merge photonics and electronics at nanoscale dimensions, and has generated intense interest in the past decade.^[2–6] Thus far, several plasmonic devices have been demonstrated, including light sources, filters, waveguides, lenses, and polarizers.^[7–12] Before applications of plasmonics can be realized, however, active plasmonic devices such as switches and modulators must be devised.^[13–18]

An effective method to achieve active plasmonics is to surround metal nanostructures with materials that have tunable optical properties (such as refractive index).^[19] Leroux et al. showed experimentally that by electrochemically changing the refractive index of polyaniline thin films, the shape and position of the localized surface plasmon resonance (LSPR) of the embedded Au nanoparticles can be reversibly tuned.^[20] Wang et al. demonstrated the electrochemical tuning of the LSPR of Ag nanoparticle arrays that were coated with WO₃ sol-gel.^[21]

Liquid crystals (LCs) can serve as excellent materials for active plasmonics, owing to their large and controllable birefringence.^[22–25] Thus far, LC-based active tuning of metal nanostructures' LSPR has been demonstrated by way of an electro-optical mechanism, in which the phase transformation of the LCs was controlled by an electric field.^[22,23,26–28] In this Communication, we present an all-optical plasmonic switch that is based on photoresponsive LCs. Upon photoirradiation, the LCs in the switch experience a phase transition and a change in their refractive index.^[29] This latter change modulates the LSPR of the embedded Au nanodisk array, because the LSPR depends on the refractive index of the surroundings. Compared with the electrically driven plasmonic switches demonstrated thus far,^[22,23,26–28] the light-driven plasmonic switches have several advantages: they could have

faster operation speeds; light can be used for dual purposes: inducing (writing) as well as detecting (reading) the behavior of plasmonic switches; and they can be integral components of future all-optical plasmonic circuits.

The switch consisted of photoresponsive LCs sandwiched between a bare glass slide and an Au nanodisk array that was immobilized on a glass substrate (Fig. 1a). The distance between the two slides was controlled by depositing monodisperse glass microspheres between them (5 μm in diameter, in this case). The pump light source was a 420 nm violet laser diode (Nichia Co.). The switching behavior was recorded by measuring with a spectrometer (HR4000G-UV-NIR from Ocean Optics). The mean diameter and period of the Au nanodisks arranged in hexagonal array were (140 ± 14) nm and (320 ± 32) nm, respectively, as seen from a representative scanning electron microscopy (SEM) image (Fig. 1b). The disks were weakly coupled, as revealed by extinction measurements. To produce the Au nanodisk arrays on a glass substrate, we used nanosphere lithography (NSL) combined with two-step reactive ion etching (RIE) techniques that were reported previously.^[30]

The photoresponsive LCs were a homogeneous mixture of 70% nematic LCs (TL213, Merck), 20% 4-butyl-4'-methylazobenzene (BMAB, synthesized per Ref [16]), and 10% chiral dopant (S811, Merck). The nematic LC changed its orientation upon exposure to light, owing to the *cis-trans* photoisomerization of the azobenzene guest molecules. Initially, the doped LCs were thermally treated to be in an isotropic phase, with their azobenzenes in the *cis* configuration. Upon photoirradiation by the pump light, the azobenzenes transformed from *cis* to *trans*, inducing the phase transition of the LCs from isotropic to nematic (Fig. 1c). The phase transition changed the refractive index of the LCs' surroundings. The LSPR of the Au nanodisks was thereby modulated, due to the aforementioned dependence of the LSPR on the refractive index of the local medium. The phase transition of photoactive LCs was the underlying physical mechanism for driving the light-driven plasmonic switch.

We recorded the extinction spectra before and after we embedded the nanodisks in the LCs. The data were recorded under normal incidence of the probe light (Fig. 2a). The solid curve is the extinction spectrum of the Au nanodisk array in air, and the dashed curve is the extinction spectrum when the array was embedded in the photoresponsive LCs. Upon embedding the LCs, their extinction peak red-shifted (from 680 to 748 nm) and the intensity of the peak decreased.

[*] Prof. T. J. Huang, Dr. V. K. S. Hsiao, Y. B. Zheng, B. K. Juluri
Department of Engineering Science and Mechanics
The Pennsylvania State University
University Park, PA 16802 (USA)
E-mail: junhuang@psu.edu

[**] This work was supported by the Air Force Office of Scientific Research (AFOSR), an NSF NIRT grant (ECCS-0609128), and the Penn State Center for Nanoscale Science (MRSEC). Components of this work were conducted at the Penn State node of the NSF-funded National Nanotechnology Infrastructure Network.

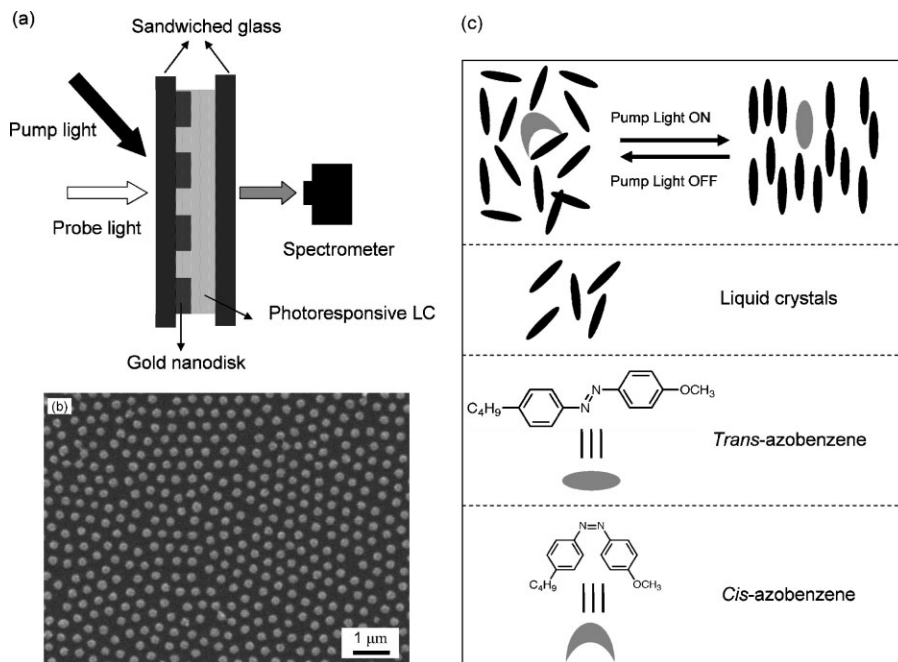


Figure 1. a) Schematic of the plasmonic switch cell. b) Scanning electron microscopy image of Au disk arrays arranged hexagonally on a glass substrate. c) Schematic of the phase transition process in photoresponsive LCs.

To understand the effects of LCs on the peak shift and intensity change, discrete-dipole approximation (DDA) calculations were carried out. We used a multilayer model in the open program DDSCAT by Draine and Flatau (version 6.1)^[27] to calculate the extinction spectra of the arrays, both before and after the Au disk array was embedded in the LCs. The model was established as follows: an isolated Au nanodisk (17 nm in thickness, 140 nm in diameter) was constructed on a glass substrate (45 nm in thickness, 140 nm in diameter, $n = 1.52$), and a Cr layer (3 nm in thickness and 140 nm in diameter) was sandwiched between the Au and the glass. The

wavelength-dependent dielectric constants for Au and Cr were obtained from Palik.^[31] LCs were modeled as a layer of dielectric material (45 nm thickness, 140 nm diameter, $n = 1.63$). Linearly polarized incident light was modeled as normal to the array. Before the LC layer was added, the calculated spectrum had a peak position at 685 nm (Fig. 2b), as compared with 680 nm for the experimental results (Fig. 2a). The spectral width, intensity, and peak position of the LSPR depended on the dipoles that were coupled between particles in the array.^[32–35] Therefore, our DDA results on isolated particles are in good agreement with the experimental results, especially considering the expected blue-shift arising from the interparticle coupling and the geometric deviations between the perfect disk used in the calculation and the actual Au disks. Based on the calculation results, we identified the measured LSPR as in-plane dipole resonance. Upon addition of the LC layer, the peak red-shifted to 751 nm in the calculated spectrum (as compared with 748 nm for the experimental results). The red-shifts of the LSPR peak in both experiments (Fig. 2a) and calculations (Fig. 2b), when air was replaced by the LCs, were caused by the increased refractive index of the surrounding media.^[36,37] The decrease in the intensity of extinction efficiency was due to the reduced scattering of the incident light by the LCs.

Extinction spectra of the Au nanodisk arrays were measured for different incident angles of the probe light (Fig. 3). When the beam was incident normal to the substrate, both the bare Au nanodisk array (Fig. 3a) and the nanodisk array embedded in the LCs (Fig. 3b) exhibited a single extinction band (which was indicative of in-plane dipole resonance). When the samples were tilted at 50° with respect to the normally incident light, an extra extinction band from the out-of-plane dipole resonance appeared at a shorter wavelength. At this angle, the out-of-plane mode was induced by the electric field normal to the substrate. When the incident angle was increased, red-shifts in the peak position of the in-plane dipole resonance were observed for both the bare and embedded Au nanodisks. The shifts could be attributed to the phase difference induced

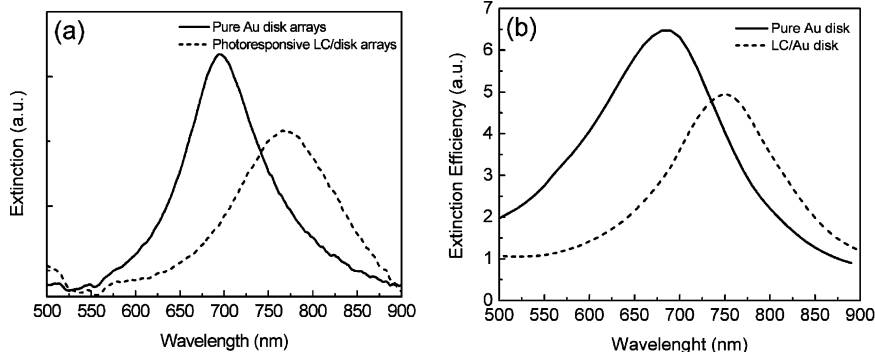


Figure 2. a) Experimental extinction spectra of a bare Au nanodisk array (solid curve) and an Au nanodisk array coated with photoresponsive LCs (dashed curve). b) Calculated extinction spectra of a bare Au nanodisk array (solid curve) and Au nanodisk array coated with photoresponsive LCs (dashed curve).

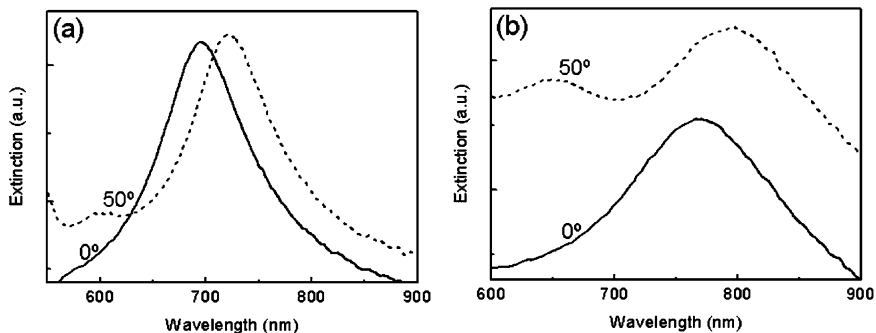


Figure 3. Extinction spectra recorded at different incident angles of probe light from a) the Au nanodisk array on glass substrate, and b) the photoresponsive LC/Au nanodisk array.

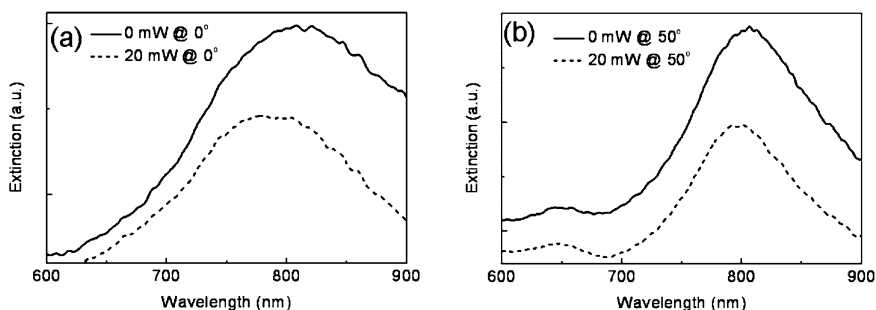


Figure 4. a) Extinction spectra of a photoresponsive LC/Au nanodisk array cell before (solid curve) and after (dashed curve) the application of an optical field from a 20 mW, 420 nm laser diode. A blue-shift ($\Delta\lambda = 30$ nm) of the extinction peak was observed. b) Similar setup, but with incident angle of probe light changed from 0° to 50° . A blue-shift of $\Delta\lambda = 10$ nm was observed.

among the coupled nanodisks when the incident light was changed from normal to the direction of tilted angle.

To demonstrate the switching effects, the cell was irradiated with a 20 mW pump light at an incident angle of 45° . A 30 nm blue-shift in the LSPR peak was observed (Fig. 4a) when the extinction spectrum was measured with the light normally incident upon the substrate. The blue-shift was reduced to 10 nm (Fig. 4b) when the probe light was 50° with respect to the normal direction of the substrate. The blue-shift of the LSPR peak was due to the decrease of the refractive index of the LCs. The different values (30 nm and 10 nm) of the blue-shift corresponding to different incident angles (0° and 50°) confirmed the preferred orientation in the LCs upon photoirradiation.

To establish the correlation between the peak shift of the LSPR and the light-induced phase transition in the photoresponsive LCs, control experiments were designed (Fig. 5a). In these experiments, the Au nanodisk arrays were outside the cell, and thus were not in contact with the sandwiched photoresponsive LCs. No peak shift of the LSPR was observed in the control experiment under the same 20 mW pump light (Fig. 5b). The intensity of the whole spectrum decreased. The decreased intensity arose from the decreased light scattering by LCs, because the molecules comprising the LCs were better-aligned upon photoirradiation.

Reversible tuning of the LSPR was achieved by switching the pump light off and on (Fig. 6). The response times for the “off” and “on” photoswitching processes were estimated to be 1.5 s and 17.1 s, respectively. Because we switched the light by blocking it manually, the measured values for the time constant do not reflect the intrinsic speed of the photoswitching processes. The response time of the azobenzene-doped LCs can be determined by multiple factors, including topology of substrate, the amount of azobenzenes, working temperature, and power of the pump light. Future work will investigate the effects of these factors on response time, and optimize these factors to achieve the intrinsic response time (on the order of microseconds) of the photoresponsive LCs.^[37]

Finally, we studied the percentage change in extinction efficiency as a function of wavelength of the incident light (Fig. 7a) and the shift of the LSPR peak as a function of the power of the pump light (Fig. 7b). The negative value of extinction efficiency suggests

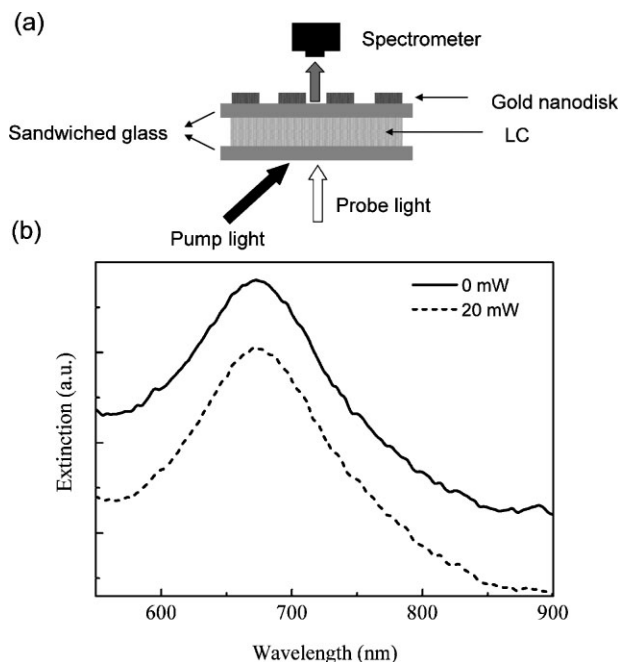


Figure 5. a) Schematic of the control experimental setup. The side with Au nanodisk arrays was outside the cell and, thus, the disks were not in contact with the sandwiched photoresponsive LCs. b) Extinction spectra of the controlled cell under external optical field of a 20 mW, 420 nm laser diode.

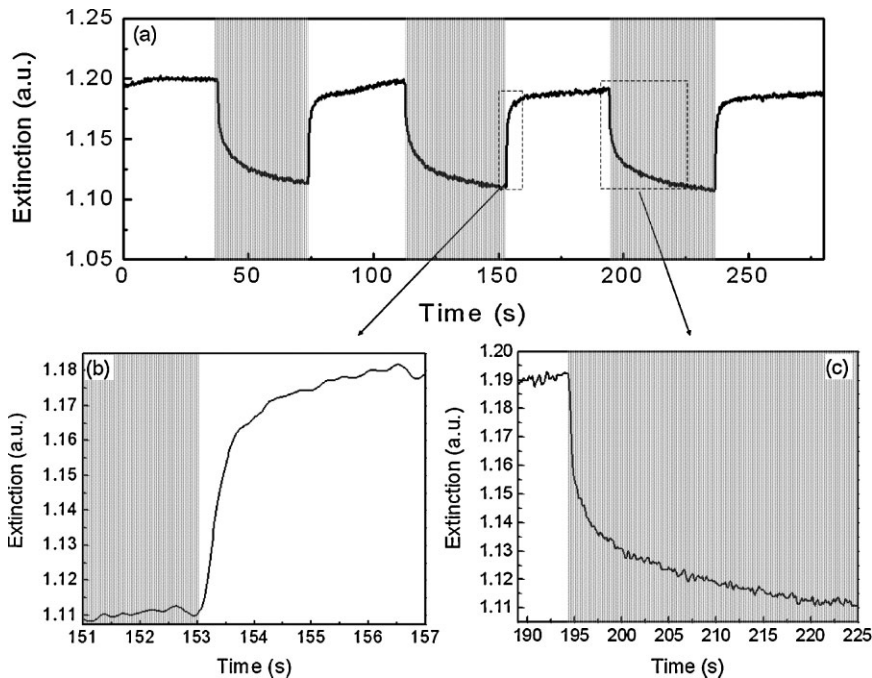


Figure 6. a) Time dependence of extinction efficiency (at a track wavelength of 725 nm) for Au nanodisks embedded in the photoresponsive LCs, when the pump light was turned on and off alternatively. b,c) Close-ups of parts of the curve shown in (a).

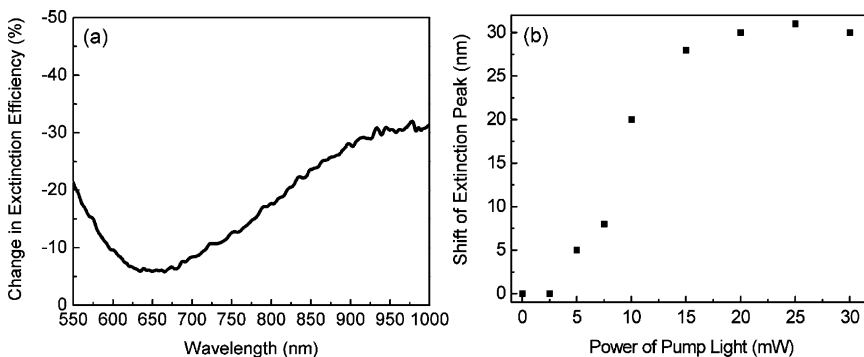


Figure 7. a) Change in extinction efficiency as a function of wavelength of incident light; b) shift of LSPR peak as a function of the power of the pump light.

a decrease in extinction after photoirradiation. The wavelength corresponding to maximum change in extinction can be tuned by choosing Au disks with different LSPR peaks. A threshold power of 2.5 mW was observed. Above the threshold, the shift increased linearly with the power, and saturated at a power of 15 mW.

In summary, we have demonstrated an all-optical plasmonic switch that is driven by Au nanodisk arrays embedded in photoresponsive LCs. As a light source incident upon the arrays was turned on and off, reversible tuning of the LSPR of the disks was achieved. By controlling the power of the external light stimulus, the peak position of the LSPR was continuously modulated. Both angle-dependence experiments

and theoretical analyses indicate that the large birefringence of nematic LCs, induced by the reversible *cis-trans* deformation of azobenzene under external light stimulus, is the underlying mechanism for the modulation in the environmental refractive index and the LSPR. This demonstration contributes to the emerging field of plasmonics, and it will prove useful in applications such as high-density optical storage devices, optical filters, and plasmonic circuits.

Received: January 7, 2008
Revised: February 18, 2008
Published online: August 5, 2008

- [1] H. Raether, *Excitation of Plasmons and Interband Transitions by Electrons*, Springer, Berlin **1980**.
- [2] V. M. Shalaev, S. Kawata, *Nanophotonics with Surface Plasmons*, Elsevier, Oxford **2007**.
- [3] S. A. Maier, *Plasmonics: Fundamental and Applications*, Springer, New York **2007**.
- [4] E. Ozbay, *Science* **2006**, *311*, 189.
- [5] S. A. Maier, M. L. Brongersma, P. G. Kik, S. Meltzer, A. A. G. Requicha, H. A. Atwater, *Adv. Mater.* **2001**, *13*, 1501.
- [6] H. A. Atwater, S. Maier, A. Polman, J. A. Dionne, L. Sweatlock, *MRS Bull.* **2005**, *30*, 385.
- [7] T. W. Ebbesen, H. J. Lezec, H. F. Ghaemi, T. Thio, P. A. Wolff, *Nature* **1998**, *391*, 667.
- [8] C. Genet, T. W. Ebbesen, *Nature* **2007**, *445*, 39.
- [9] N. Fang, H. Lee, C. Sun, X. Zhang, *Science* **2005**, *308*, 534.
- [10] H. J. Lezec, A. Degiron, E. Devaux, R. A. Linke, L. Martin-Moreno, F. J. Garcia-Vidal, T. W. Ebbesen, *Science* **2002**, *297*, 820.
- [11] Z. W. Liu, H. Lee, Y. Xiong, C. Sun, X. Zhang, *Science* **2007**, *315*, 1686.
- [12] M. Quinten, A. Leitner, J. R. Krenn, F. R. Aussenegg, *Opt. Lett.* **1998**, *23*, 1331.
- [13] J. G. Rivas, M. Kuttge, H. Kurz, P. H. Bolivar, J. A. Sanchez-Gil, *Appl. Phys. Lett.* **2006**, *88*, 082106.
- [14] A. V. Krasavin, N. I. Zheludev, *Appl. Phys. Lett.* **2004**, *84*, 1416.
- [15] P. Andrew, W. L. Barnes, *Science* **2004**, *306*, 1002.
- [16] B. K. Juluri, Y. B. Zheng, D. Ahmed, L. Jensen, T. J. Huang, *J. Phys. Chem. C* **2008**, *112*, 7309.
- [17] S. I. Bozhevolnyi, V. S. Volkov, E. Devaux, J. Y. Laluet, T. W. Ebbesen, *Nature* **2006**, *440*, 508.
- [18] J. Dintinger, S. Klein, T. W. Ebbesen, *Adv. Mater.* **2006**, *18*, 1267.
- [19] M. Maaza, O. Nemraoui, C. Sella, A. C. Beye, B. Baruch-Barak, *Opt. Commun.* **2005**, *254*, 188.
- [20] Y. R. Leroux, J. C. Lacroix, K. I. Chane-Ching, C. Fave, N. Felidj, G. Levi, J. Aubard, J. R. Krenn, A. Hohenau, *J. Am. Chem. Soc.* **2005**, *127*, 16022.
- [21] Z. C. Wang, G. Chumanov, *Adv. Mater.* **2003**, *15*, 1285.

- [22] P. A. Kossyrev, A. J. Yin, S. G. Cloutier, D. A. Cardimona, D. H. Huang, P. M. Alsing, J. M. Xu, *Nano Lett.* **2005**, *5*, 1978.
- [23] K. C. Chu, C. Y. Chao, Y. F. Chen, Y. C. Wu, C. C. Chen, *Appl. Phys. Lett.* **2006**, *89*, 103107.
- [24] J. Muller, C. Sonnichsen, H. von Poschinger, G. von Plessen, T. A. Klar, J. Feldmann, *Appl. Phys. Lett.* **2002**, *81*, 171.
- [25] W. Dickson, G. A. Wurtz, P. R. Evans, R. J. Pollard, A. V. Zayats, *Nano Lett.* in press
- [26] P. R. Evans, G. A. Wurtz, W. R. Hendren, R. Atkinson, W. Dickson, A. V. Zayats, R. J. Pollard, *Appl. Phys. Lett.* **2007**, *91*, 043101.
- [27] S. Y. Park, D. Stroud, *Phys. Rev. Lett.* **2005**, *94*, 217401.
- [28] Y. Wang, *Appl. Phys. Lett.* **1995**, *67*, 2759.
- [29] T. Ikeda, *J. Mater. Chem.* **2003**, *13*, 2037.
- [30] Y. B. Zheng, B. K. Juluri, X. L. Mao, T. R. Walker, T. J. Huang, *J. Appl. Phys.* **2008**, *103*, 014308.
- [31] E. D. Palik, *Handbook of Optical Constants of Solids*, Academic, New York **1985**.
- [32] L. L. Zhao, K. L. Kelly, G. C. Schatz, *J. Phys. Chem. B* **2003**, *107*, 7343.
- [33] E. M. Hicks, S. L. Zou, G. C. Schatz, K. G. Spears, R. P. Van Duyne, L. Gunnarsson, T. Rindzevicius, B. Kasemo, M. Kall, *Nano Lett.* **2005**, *5*, 1065.
- [34] S. L. Zou, N. Janel, G. C. Schatz, *J. Chem. Phys.* **2004**, *120*, 10871.
- [35] B. Lamprecht, G. Schider, R. T. Lechner, H. Ditlbacher, J. R. Krenn, A. Leitner, F. R. Aussenegg, *Phys. Rev. Lett.* **2000**, *84*, 4721.
- [36] Y. B. Zheng, T. J. Huang, A. Y. Desai, S. J. Wang, L. K. Tan, H. Gao, A. C. H. Huan, *Appl. Phys. Lett.* **2007**, *90*, 183117.
- [37] A. Shishido, O. Tsutsumi, A. Kanazawa, T. Shiono, T. Ikeda, N. Tamai, *J. Am. Chem. Soc.* **1997**, *119*, 7791.